



Research Article

Study on the Factors Influencing on Wetting Performance of Blasting Dust in a Limestone Mine

Jinrui Nie ¹, Shujie Yuan ^{1,2}, Ye Li,³ and Xiaoming Huang³

¹School of Safety Science and Engineering, Anhui University of Science and Technology, Huainan, Anhui 232001, China

²Key Laboratory of Safe and Effective Coal Mining, Ministry of Education, Huainan, Anhui 232001, China

³Anhui Conch Cement Co., Ltd., Wuhu, Anhui 241000, China

Correspondence should be addressed to Shujie Yuan; yuansj@aust.edu.cn

Received 16 October 2022; Revised 16 November 2022; Accepted 29 November 2022; Published 16 December 2022

Academic Editor: Hetang Wang

Copyright © 2022 Jinrui Nie et al. This is an open access article distributed under the Creative Commons Attribution License, which permits unrestricted use, distribution, and reproduction in any medium, provided the original work is properly cited.

In order to find out the factors influencing on wetting performance of blasting dust in open-pit limestone mines, the blasting dusts in a limestone mine in Tongling, Anhui Province, were studied. The samples of hydrophobic dust (MD) and hydrophilic dust (ND) were obtained by hydrostatic separation experiment. The contact angle of water on dust samples, particle size distribution, surface oxygen-containing functional groups, surface mineral composition and content, and surface pore structure was determined. The measurement results of contact angle indicate that the wetting performance of MD is weaker than that of ND. By comparative analyzing, the surface characteristics of MD and ND factors influencing on the wetting performance of the dusts were determined. The results showed that MD has a smaller particle size, higher volume fraction of hydrophobic groups, and more complex surface morphology than that of ND, which leads to its weaker wetting performance than that of ND.

1. Introduction

In the process of exploitation in open-pit limestone mines, a large amount of dust is emitted in the blasting operation [1]. The blasting dust not only increase the prevalence of pneumoconiosis among miners but also pollute atmospheric environment [2]. The gases produced by explosive explosion include CO₂, CO, N₂, and NO_x [3]. The blasting, crushing, and other processes in the mining process have direct impact on the physicochemical characteristics of dust. The greater the energy consumed in the production process, the smaller the dust particle size, and the more complex the pore structure, which leads to the weaker wetting performance of dust [4]. The characteristics of blasting dust, such as high concentration, easy diffusion, wide pollution range, and easy to cause secondary pollution, make the dust suppression effect difficult to be improved [5]. Strengthening the research of

blasting dust control technology in open-pit mines is in line with the new trend of building green mines.

Lots of means have been developed to suppress blasting dust. Liu et al. and Yang et al. [6, 7] studied the influencing factors of blasting dust emission and put forward using water mist to suppress blasting dust emission. Wang et al. and Jin et al. [8, 9] developed chemical dust suppressants based on the study of the characteristics of blasting dust and suppressed dust through water-sealed blasting. Hosseini et al. [10] optimized blasting parameter to depress the blasting dust emission. In the blasting construction of tunnels and underground mine, ventilation and spraying are used to suppress dust [11]. At present, the use of wet dedusting is the most widespread, and the dust wetting performance to a large extent determines its dedusting efficiency [12]. Studies [13–15] found that the wetting performance of dust is significantly influenced by its surface physicochemical

characteristics. Usually, the wetting performance of dust is directly characterized by the contact angle of water on the dust surface; the bigger the contact angle, the weaker the wetting performance of dust [16]. Fu et al. [17] analyzed the composition of the blasting dust produced in the course of blasting demolition of urban buildings and considered that the cracks and microstructure of the blasting dust were the main reasons for its hydrophobicity. Xu et al.'s research [18] shows that the wetting performance of dust is greatly affected by its particle size, and its hydrophobicity increases apparently with the decrease of particle size. The hydrophilic mineral composition of the dust surface can significantly improve its wetting performance, the common hydrophilic mineral such as calcite (CaCO_3) and quartz (SiO_2) [19]. The surface carbon-containing functional groups of dust apparently affect its wetting performance, which carbon-containing macromolecular structures show strong hydrophobicity of coal dust due to a large amount of surface content of carbon-containing macromolecular groups such as fatty hydrocarbons and aromatic hydrocarbons, which leads to the weak wetting performance [20–22]. Study [23] analyzed the impact of surface pore structure of dust on its wetting performance, indicating that the complex surface pore structure leads to hydrophobicity. According to Xiazhong et al. [24], the blasting dust with higher water content is more likely to produce condensation effect when it is in contact with water, thus showing hydrophilicity.

As has been shown, lots of studies of dust surface characteristics influencing on its wetting performance have been conducted and some achievements have been made. However, the studies are mainly focused on coal and metal mine dust; the study of limestone mine dust needs to be further enriched. This study determined the factors affecting the wetting performance of limestone mine dust and provide theoretical support for the suppression of blasting dust.

2. Materials and Methods

2.1. The Preparation of Dust Sample. The blasting dust sample separated using a 200 mesh ($74\ \mu\text{m}$) was dried at 60°C in an incubator for 8 h, and then cooled at 25°C for use. As shown in Figure 1, the prepared blasting dust was poured into a beaker containing deionized water (surface tension of $73.02\ \text{mN/m}$). After one minute, no more dust settling to the bottom of the cup, and the blasting dust sample was separated into two different parts. The dust floating on the surface is nonwet dust, called hydrophobic blasting dust (MD), and which dust deposited on the bottom of beaker is wetted dust, called hydrophilic blasting dust (ND). Each part of the dusts was picked up and dried in an incubator at 120°C for 2 h.

2.2. Wetting Performance Test. The contact angles of deionized water on the surface of MD and ND were measured using a contact angle apparatus (OCA20). The dusts were pressed into tablet-shaped samples, under the pressure of $50\ \text{MPa}$ for 5 min. The experimental steps are as follows: the deionized water was dripped on the surface of the blasting dust samples consecutively and slowly with a syringe

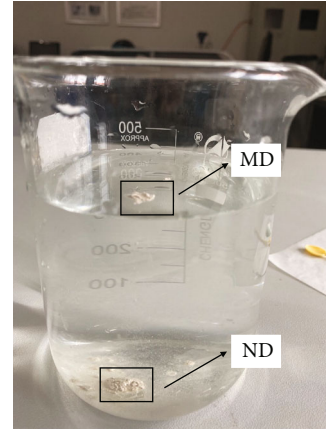


FIGURE 1: Hydrostatic separation experiment of MD and ND.

needle. The whole process of droplets contacting the surface of the dust samples was recorded dynamically by using SCA20 software. After adjusting the baseline, the change of the contact angle of water on the dust samples with time was obtained. The same dust sample was measured twice and the average value of the results was taken as the final result.

2.3. Physical Properties Test

2.3.1. Particle Size Distribution Test. The laser particle size analyzer Malvern Mastersizer 2000 was used to measure the particle size distributions of MD and ND. Water was selected as the dispersive solution, and the bubbles in the dispersive solution were blown by ultrasound before the test. Dust samples were slowly added after the background value was deducted. The same dust sample was measured twice and the average value of the results was taken as the final result.

2.3.2. Pore Structure Measurement. The Micromeritics ASAP 2460 fully automatic specific surface and porosity analyzer BET was used to analyze the pore structures of the MD and ND, using the nitrogen adsorption method, under condition of temperature set at 120°C and degassing time of 12 h.

2.4. Chemical Properties Test

2.4.1. XRD Analysis. The surface mineral composition and content of MD and ND were measured by X-ray diffraction (XRD). Dust sample was placed on glass slides; the surface mineral composition of MD and ND was determined by X-ray diffractometer, using a $\text{Cu-K}\alpha$ radiation source with the working voltage of $40\ \text{kV}$ and working current of $40\ \text{mA}$. The diffraction angles were from 2° to 100° with angular speed of $2^\circ/\text{min}$. The data were analyzed using software MDI Jade 6.1, and the adiabatic method was used to conduct the semiquantitative analysis of the phase in the dust samples.

2.4.2. XPS Analysis. The X-ray photoelectron spectroscopy (XPS) was used to measure the surface carbon-containing macromolecular groups of MD and ND. In the XPS test,

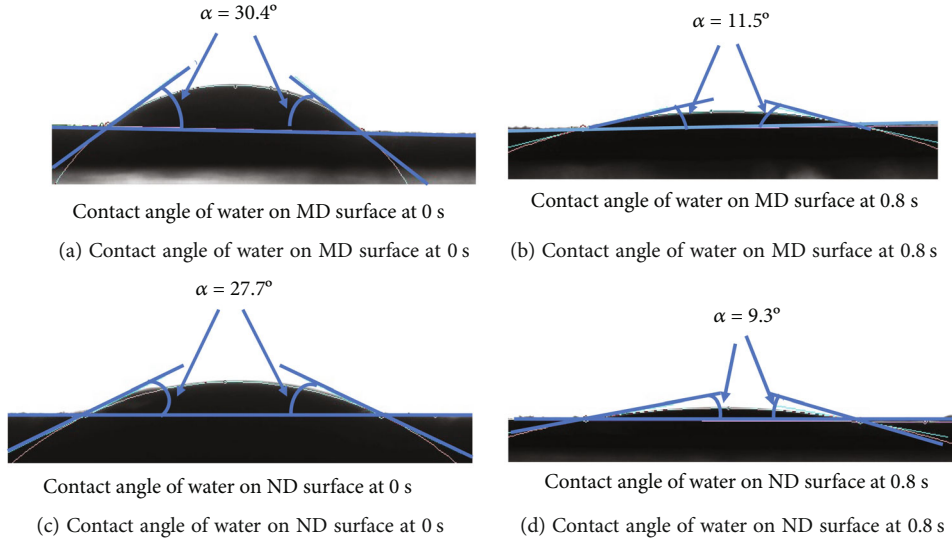


FIGURE 2: Contact angles of water on the surface of MD and ND at the beginning and the ending of the test.

the sample chamber pressure was less than 2.0×10^{-7} mbar, the spot size was $400 \mu\text{m}$, the operating voltage was 12 kV, and the filament current was 6 mA. The full-spectrum scanning energy is 150 eV and the step length is 1 eV. The narrow-spectrum scanning energy was 50 eV and the step length is 0.1 eV. The binding energy was corrected by C1s peak with the reference value of 248.8 eV.

3. Results and Discussion

3.1. Wetting Performance Analysis. The contact angles of deionize water on MD and ND surface at the beginning and the ending of the test are shown in Figure 2, and the changes of the contact angles of MD and ND with time are shown in Figure 3. The contact angles of MD and ND surface gradually decreased with the increase of time. The contact angles of MD and ND, respectively, decreased from 30.4° and 27.7° to 11.5° and 9.3° . The contact angles of ND decreased more significantly. The contact angle of MD is always larger than on ND. Thus, the wetting performance of MD is weaker than that of ND. This conclusion is consistent with the result of the hydrostatic separation experiment.

3.2. Particle Size Distribution Analysis. The test results of the particle size distribution of MD and ND are shown in Figure 4, and the cumulative distribution percentage of MD and ND in different particle size intervals is shown in Table 1. The particle size distributions of MD and ND are quite different. Among them, the proportion of slight dust below $10 \mu\text{m}$ in MD is 10.81% higher than ND. The percentage of MD is 28.41% higher than ND in the particle size distribution range below $20 \mu\text{m}$.

The physical parameters of MD and ND are shown in Table 2. D_{10} , D_{50} , and D_{90} indicate the particle size of dusts when the cumulative particle size distribution arrives 10%, 50%, and 90%, respectively. $D_{(4,3)}$ represents the volume-weighted average particle size [25]. As shown in

Table 2, all parameters of ND are bigger than those of MD, and the mass specific surface area of MD and ND is $1.523 \text{m}^2 \cdot \text{g}^{-1}$ and $0.726 \text{m}^2 \cdot \text{g}^{-1}$, respectively. Study [26] showed that the smaller the particle size and the larger the mass specific surface area of dust, the stronger the surface energy and surface activity of the dust and the harder it is to be wetted. Therefore, the wetting performance of MD is weaker than that of ND.

3.3. Analysis of Surface Pore Structure. When water touches the dust, actual contact area on the dust surface will be larger than the apparent contact area, so the surface will increase its wetting performance [27]. The difference in structure between MD and ND surface was quantitatively analyzed by N_2 adsorption at low temperature.

The low-temperature N_2 adsorption isotherms of MD and ND are shown in Figure 5. At the liquid N_2 temperature (77 K), the amount of N_2 adsorption on the dust surface depends on the relative pressure of nitrogen (p/p_0); “ p ” is the partial pressure of N_2 and “ p_0 ” is the saturated vapor pressure of N_2 at the liquid nitrogen temperature. Depending on the characteristics of the hysteresis loop of the low-temperature N_2 adsorption isotherm, it can be divided into slit-shaped, cylindrical, wedge-shaped, and ink-bottle-shaped types [28]. The low-temperature N_2 adsorption isotherms of MD and ND are more consistent with the wedge-shaped adsorption isotherm, which indicates that there are many closed or semiclosed pores on the dust surface. The maximum N_2 adsorption volume of MD is $4.50 \text{cm}^3 \cdot \text{g}^{-1}$, which is higher than that of ND ($4.09 \text{cm}^3 \cdot \text{g}^{-1}$). Therefore, the surface pore structure of MD is more developed, and its adsorption capacity to N_2 is stronger.

The specific surface areas (SSAs) of MD and ND were characterized by Langmuir (L) and Brunauer-Emmett-Teller (BET) according to the pore size classification of powder materials. The pore volume of the two kinds of dusts was calculated by Dubinn-Radushkevich (D-R) and

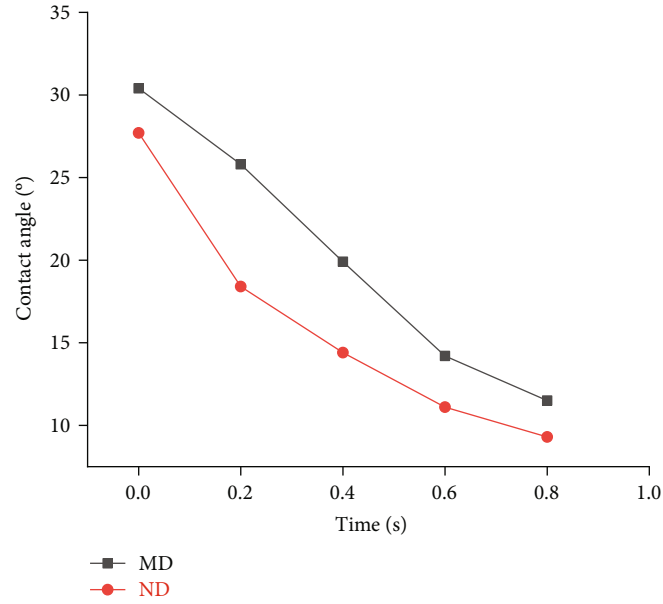


FIGURE 3: Changes of contact angle with time.

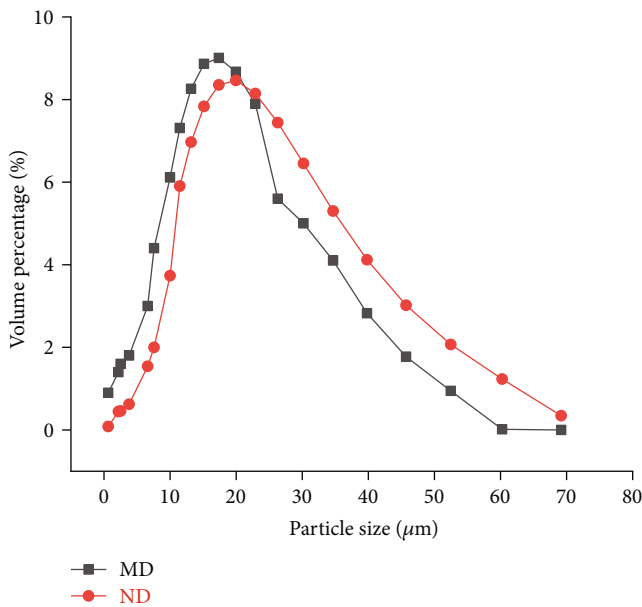


FIGURE 4: Particle size distribution of MD and ND.

Barrett-Joyner-Halenda (BJH). The pore structure parameters of the two kinds of dusts were calculated by BJH and BET methods. The pore volume and structure parameters of MD and ND are shown in Table 3. The SSA_{BET} and SSA_L of MD are 53.5% and 55.1% higher than those of ND, respectively. The total pore volume of MD is 86.6% higher than that of ND. The average pore size of MD is 32.1% smaller than that of ND. The results show that the pore structure of MD surface is more complex than that of ND.

The distributions of pore sizes and cumulative pore volumes of MD and ND are shown in Figure 6. When the pore diameter is less than 11.61 nm, the micropore volume of MD is consistently higher than that of ND, but the cumulative pore volume of MD is always higher than that of ND, which further indicates that the pore structure of MD is significantly different from that of ND. The micropore volume and cumulative pore volume on MD surface are higher than those of ND, and the pore structure of MD is more complex.

In conclusion, MD has complex pore structure than ND. Because of the complex pore structure, MD has a strong adsorption ability to air, which leads to the tight air film being more likely to form on the dust surface, and hinders the contact wetting of water to dust [29]. In addition, the complex pore structure makes the specific surface area of MD larger than that of ND, which makes MD have higher surface energy and more repulsive force to water, thus hindering water from spreading and wetting on the dust surface. Therefore, the difference in the surface pore morphology between MD and ND results in the difference in their wetting performance.

3.4. XRD Analysis. The XRD patterns of MD and ND are shown in Figure 7, and the volume fractions of mineral composition of MD and ND are shown in Table 4. The XRD patterns of MD and ND are very similar, and they are mainly composed of $CaCO_3$ and SiO_2 . The volume fraction of $CaCO_3$ in MD is 99.4%, and that of SiO_2 is 0.6%. The volume fraction of $CaCO_3$ and SiO_2 in ND is 99.1% and 0.9%, respectively. The composition and content of the two kinds of dusts are basically the same. $CaCO_3$ and SiO_2 are hydrophilic minerals. Therefore, the surface mineral composition of the two dusts is not the factor causing the difference in their wetting performance.

TABLE 1: Percentage of cumulative distribution of MD and ND in different particle size intervals.

Particle size area (μm)	0~10	10~20	20~30	30~40	40~50	50~60	60~70
MD (%)	31.08	42.11	17.16	6.92	2.27	0.01	0.00
ND (%)	20.27	24.51	22.04	12.5	8.09	1.77	0.35

TABLE 2: Physical parameters of MD and ND.

Parameter	D_{10} (μm)	D_{50} (μm)	D_{90} (μm)	$D_{(4,3)}$ (μm)	Mass specific area ($\text{m}^2 \cdot \text{g}^{-1}$)
MD	3.121	13.423	29.937	15.292	1.523
ND	5.834	16.463	41.782	19.836	0.726

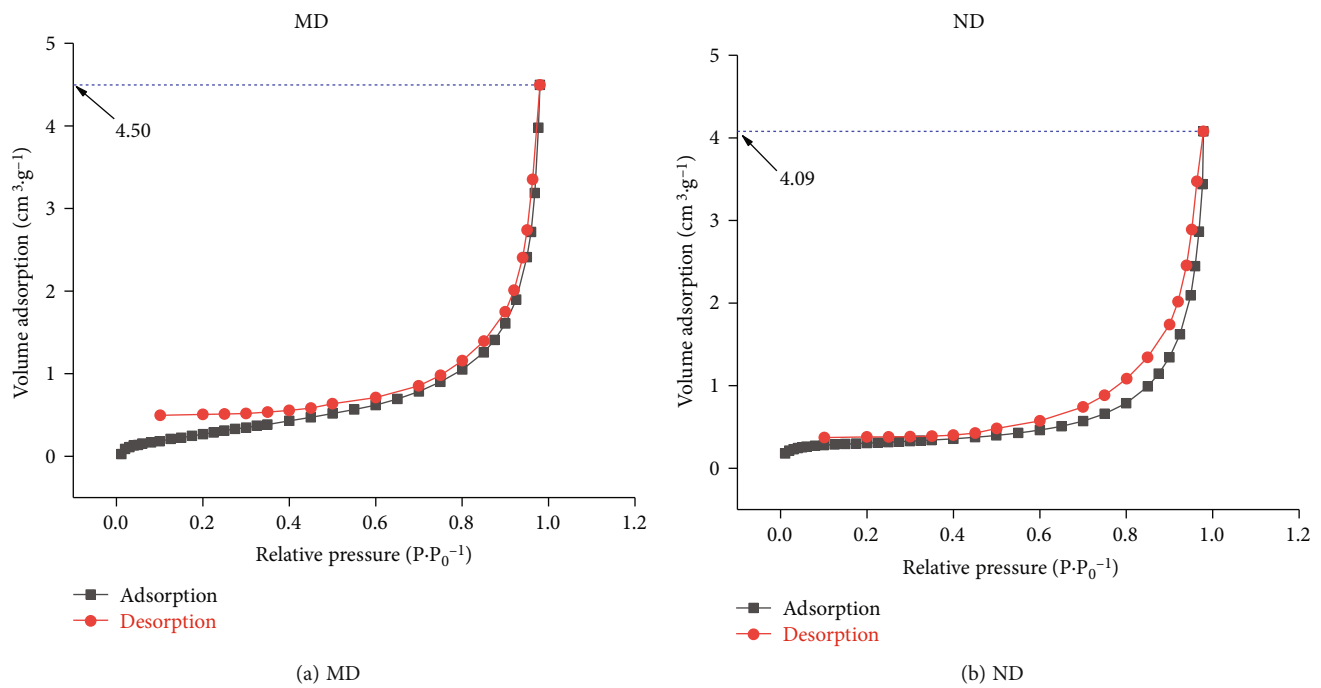


FIGURE 5: Adsorption-desorption isotherms of MD and ND.

TABLE 3: Pore volume and structure parameters of MD and ND.

Dust sample	SSA ($\text{m}^2 \cdot \text{g}^{-1}$)		Pore volume ($\text{cm}^3 \cdot \text{g}^{-1}$)			Pore size (nm)
	SSA_{BET}	SSA_{L}	BJH ^a volume	D-R ^b volume	Total volume	BJH (average pore size)
MD	6.34	9.68	0.0116	0.0011	0.0127	17.5434
ND	4.13	6.24	0.0067	0.0000	0.0067	25.8414

Note: a: mesopore volume, b: microhole volume, and total volume = mesopore volume + microhole volume.

3.5. XPS Analysis. The XPS test patterns of the MD and ND were charge-corrected using C(1s) for the standard peak position (284.8 eV), and the reference peak positions of each element were aligned with the standard peak positions; the main occurrence forms of C on the dusts surfaces can be obtained [30]. The C(1s) XPS spectra of MD and ND surface are shown in Figure 8. It can be seen in Figure 8 that

there are five major groups on the surface of MD and ND, which are C-C C-OR, O-C=O, C-H, and C=O. The contents of the bound state of the elements are represented by the peak area of the spectra. The binding energy and percentage of the relative peak areas of the components on the surface of MD and ND dusts obtained from XPS analysis of C(1s) are shown in Table 5.

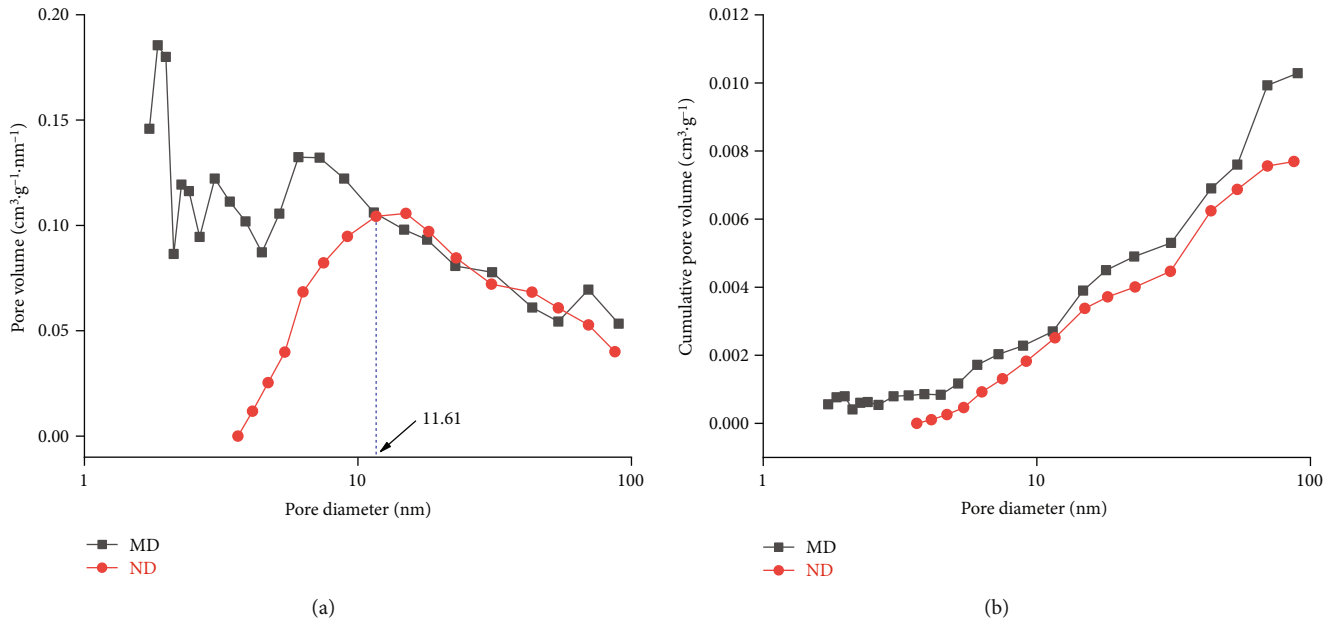


FIGURE 6: The distributions of pore sizes and cumulative pore volumes of MD and ND.

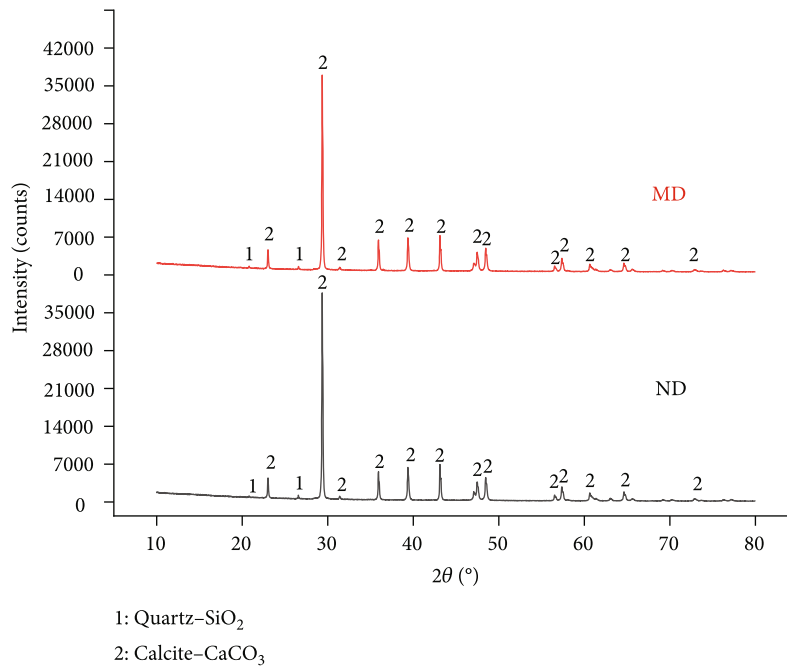


FIGURE 7: XRD patterns of MD and ND.

TABLE 4: Volume fraction of mineral composition in MD and ND.

Mineral composition	CaCO ₃	SiO ₂
MD (%)	99.4	0.6
ND (%)	99.1	0.9

C-C and C-H show hydrophobic; C-OR, C=O, and O-C=O show hydrophilic [31]. According to Table 5, the volume fractions of hydrophobic groups and hydrophilic

groups on MD surface are 57.21% and 42.79%, respectively. The volume fractions of hydrophobic groups and hydrophilic groups on ND surface are 36.82% and 63.18%, respectively. The volume fraction of hydrophobic groups on MD surface is 20.39% higher than that of ND, and the volume fraction of hydrophilic groups is 20.39% lower than that of ND, which is consistent with the conclusion that the wetting performance of ND is stronger than that of MD. Therefore, the surface groups of the dusts affect their wetting performance.

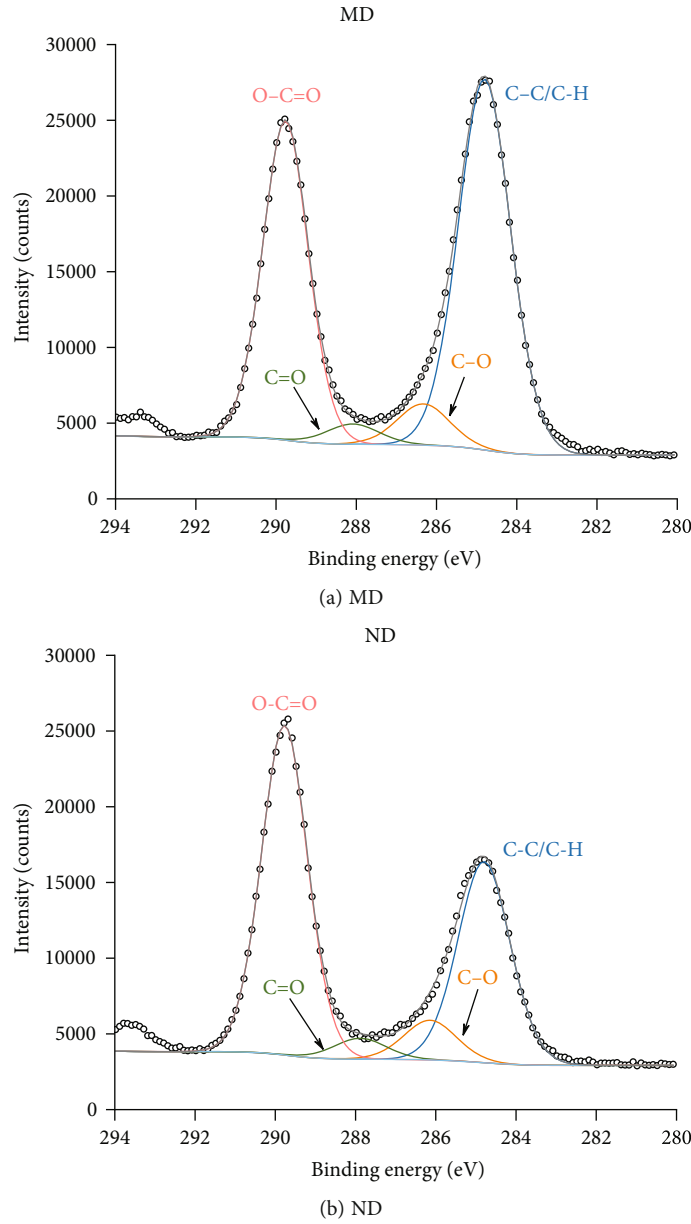


FIGURE 8: C(1 s) XPS spectra of MD and ND surface.

TABLE 5: The binding energy and percentage of the relative peak areas of the components on the dust surface of MD and ND obtained from XPS analysis of C(1 s).

Dust sample	C-C/C-H		C-OR		C=O		O-C=O	
	E_B (eV)	φ (%)	E_B (eV)	φ (%)	E_B (eV)	φ (%)	E_B (eV)	φ (%)
MD	284.8	57.21	286	5.82	287	3.85	289.8	33.12
ND	284.8	36.82	286	6.18	287	4.37	289.8	52.63

4. Conclusions

(1)The surface area of MD is $0.797 \text{ m}^2 \cdot \text{g}^{-1}$ larger than that of ND. Due to the smaller particle size and more complex surface morphology, the specific surface area and surface energy of MD are larger, which prevents the dust from being wetted

by water and makes the wetting performance of MD weaker than that of ND

(2)The pore structure in MD surface is more complex than that in ND surface. The average pore size in MD surface is 8.298 nm lower than that in ND surface, and the total pore volume in MD surface is 1.90 times higher than that in

ND surface. The complex surface morphology results in easier forming the air film on the surface of MD and reduces its wetting performance

(3) The volume fractions of hydrophilic groups in the surface of MD and ND are 42.79% and 63.18%, respectively. The volume fractions of hydrophobic groups in the surface of MD and ND are 57.21% and 36.82%, respectively. The volume fraction of hydrophilic groups in the surface of MD is less than that in ND surface, and the volume fraction of hydrophobic groups is larger than that in ND surface, which results in weak wetting performance of MD

Data Availability

The data can be obtained by contacting the corresponding author directly.

Conflicts of Interest

The authors declare that there is no conflict of interest regarding the manuscript.

Acknowledgments

This study was supported by the Project “Construction of the Key Laboratory of Safe and Effective Coal Mining, Ministry of Education, China” and “the Joint Training Graduate Student Program of Anhui University of Science and Technology and Anhui Conch Cement Co., Ltd.”

References

- [1] C. F. Du and S. Chen, “Analysis on dust resource intensification for open-pit mines and experimental study on the contribution rate,” *Industrial Safety and Environmental Protection*, vol. 40, no. 10, pp. 76–79, 2014.
- [2] Z. Xie, Y. Xiao, C. Jiang, Z. Ren, X. Li, and K. Yu, “Numerical study on fine dust pollution characteristics under various ventilation time in metro tunnel after blasting,” *Building and Environment*, vol. 40, no. 10, pp. 76–79, 2014.
- [3] C. Y. Zhang, “Research on toxic gas of industrial explosive explosion and its influencing factors,” *Coal Mine blasting*, vol. 40, no. 3, pp. 16–19, 2022.
- [4] J. S. Chen, N. Jiang, and Z. A. Jiang, “Numerical simulation of dust distribution and influencing factors in slope drilling,” *Chinese Journal of Engineering*, vol. 40, no. 6, p. 692, 2015.
- [5] Z. Zhang, Y. J. Tong, Z. H. Li, H. Q. Bai, and J. Z. Liu, “The experiment of using explosion water reduce dust in the bench blasting of open-pit mine,” *Engineering Blasting*, vol. 23, no. 5, pp. 71–75, 2014.
- [6] J. Liu, Z. Li, H. Bai, T. Cao, and Z. Chen, “Research on influence factors of blasting dust emission of open-pit mine,” *Blasting*, vol. 34, no. 4, pp. 169–174, 2017.
- [7] N. H. Yang, Y. Guo, H. Q. Bai, and Z. Zhang, “Experimental study on dust suppression by explosion water mist in open bench blasting,” *Blasting*, vol. 38, no. 3, pp. 130–135, 2021.
- [8] Y. Wang, C. Du, J. Wang, and H. Li, *Chemical Suppression Technology of Open-Pit Mine Blasting Dust and Smoke*, Springer, Singapore, 2022.
- [9] L. Z. Jin, J. G. Liu, and M. Yu, “Dust reduction mechanism and application research of efficient water stemming,” *Journal of University of Science and Technology Beijing*, vol. 29, no. 11, pp. 1079–1082, 2007.
- [10] S. Hosseini, S. Monjezi, and E. Bakhtavar, “Minimization of blast-induced dust emission using gene-expression programming and grasshopper optimization algorithm: a smart mining solution based on blasting plan optimization,” *Clean Technologies and Environmental Policy*, vol. 24, no. 8, pp. 2313–2328, 2022.
- [11] X. T. Zhang, Y. Bai, H. M. Zhou, and H. L. Wang, “Study and application on dust comprehensive prevention and control technology in tunnel excavation by blasting,” *Advanced Materials Research*, vol. 549, pp. 931–935, 2012.
- [12] Q. Zhou and B. Qin, “Coal dust suppression based on water mediums: a review of technologies and influencing factors,” *Fuel*, vol. 302, article 121196, 2021.
- [13] Q. Zhou, B. Qin, J. Wang, H. Wang, and F. Wang, “Experimental investigation on the changes of the wettability and surface characteristics of coal dust with different fractal dimensions,” *Colloids and Surfaces A: Physicochemical and Engineering Aspects*, vol. 551, pp. 148–157, 2018.
- [14] B. Zhao, S. G. Li, H. F. Lin, Y. Cheng, X. Kong, and Y. Ding, “Experimental study on the influence of surfactants in compound solution on the wetting-agglomeration properties of bituminous coal dust,” *Powder Technology*, vol. 395, pp. 766–775, 2022.
- [15] Q. Z. Li, B. Q. Lin, S. Zhao, and H. Dai, “Surface physical properties and its effects on the wetting behaviors of respirable coal mine dust,” *Powder Technology*, vol. 233, pp. 137–145, 2013.
- [16] G. Zhou, H. Qiu, Q. Zhang, M. Xu, J. Wang, and G. Wang, “Experimental investigation of coal dust wettability based on surface contact angle,” *Journal of Chemistry*, vol. 2016, Article ID 9452303, 8 pages, 2016.
- [17] J. T. Fu, L. L. Hu, and M. H. Hu, “Investigating blasting demolition dust micromorphology, microscopic agglomeration process with wetting droplet and suppression effectiveness by explosion water mist,” *Frontiers in Environmental Science*, vol. 37, no. 6, pp. 685–692, 2015.
- [18] C. Xu, D. Wang, H. Wang et al., “Effects of chemical properties of coal dust on its wettability,” *Powder Technology*, vol. 318, pp. 33–39, 2017.
- [19] P. Wang, X. Tan, L. Zhang, Y. Li, and R. Liu, “Influence of particle diameter on the wettability of coal dust and the dust suppression efficiency via spraying,” *Process Safe Environment Protect*, vol. 132, pp. 189–199, 2019.
- [20] Z. Zhu, R. Cong, L. Zhou, H. Zheng, Y. Tu, and Z. Wu, “Effects of chemical properties and inherent mineral matters on pyrolysis kinetics of low-rank coals,” *Processes*, vol. 9, no. 12, 2021.
- [21] H. T. Wang, L. Zhang, D. M. Wang, and X. He, “Experimental investigation on the wettability of respirable coal dust based on infrared spectroscopy and contact angle analysis,” *Advanced Powder Technology*, vol. 28, no. 12, pp. 3130–3139, 2017.
- [22] W. Zhang, Q. Hu, S. Jiang, L. Wang, J. Chai, and J. Mei, “Experimental study on coal dust wettability strengthened by surface active ionic liquids,” *Environmental Science and Pollution Research International*, vol. 29, no. 30, 2022.
- [23] J. Zhang, H. Li, Y. Liu et al., “Micro-wetting characteristics of coal dust and preliminary study on the development of dust suppressant in Pingdingshan mining area,” *Journal of China Coal Society*, vol. 46, no. 3, pp. 812–825, 2021.
- [24] Z. Xiazhong, Y. Qiu, J. Lianghai, Z. H. E. N. G. Yuhang, L. U. O. Han, and M. A. Guofeng, “Numerical simulation on

- spatio-temporal distribution regularities of blasting dust mass concentration in open quarry,” *China Safety Science Journal*, vol. 30, no. 10, pp. 55–62, 2018.
- [25] C. F. Wang, S. Q. Lu, S. F. Si, and M. J. Li, “Study on influence of magnetization effect on water properties and optimization,” *Journal of Safety Science and Technology*, vol. 18, no. 4, pp. 141–146, 2022.
- [26] L. Jin, J. Liu, J. Guo, J. Wang, and T. Wang, “Physicochemical factors affecting the wettability of copper mine blasting dust,” *International Journal of Coal Science & Technology*, vol. 8, no. 2, pp. 265–273, 2021.
- [27] Q. Z. Li, B. Q. Lin, J. K. Zhang, J. J. Dan, and H. M. Dai, “Fractal characteristics of particle size distribution and its effects on the surface wetting performance of coal mine dusts,” *Journal of China Coal Society*, vol. 37, no. 1, pp. 138–142, 2012.
- [28] J. J. Fan, Y. W. Ju, S. B. Liu, and X. S. Li, “Micropore structure of coals under different reservoir conditions and its implication for coal-bed methane development,” *Journal of China Coal Society*, vol. 38, no. 3, pp. 441–447, 2013.
- [29] J. Y. Wang, L. Z. Jin, J. Z. Guo, J. G. Liu, T. Y. Wang, and Q. Gong, “Key influencing factors on wettability of blasting dust in Meishan iron mine,” *Journal of Central South University (Science and Technology)*, vol. 50, no. 10, pp. 2527–2535, 2019.
- [30] J.-g. Liu, L.-z. Jin, J.-y. Wang, S.-n. Ou, J.-z. Ghio, and T.-y. Wang, “Micromorphology and physicochemical properties of hydrophobic blasting dust in iron mines,” *International Journal of Minerals, Metallurgy, and Materials*, vol. 26, no. 6, 2019.
- [31] L. Jin, J. Wang, and J. Liu, “Influence of the surface features of the inlet dust in Luoshan mountain gold mine on its wettability,” *Journal of Safety and Environment*, vol. 19, no. 6, pp. 1954–1962, 2019.